

The Implication of Heat and Water Balance Changes in a Lake Basin on the Tibetan Plateau

Jianqing Xu¹, Shumei Yu², Jingshi Liu², Shigenori Haginoya³, Yasushi Ishigooka⁴,
Tsuneo Kuwagata⁴, Masayuki Hara¹, and Tetsuzo Yasunari^{1,5}

¹Frontier Research Center for Global Change, Japan Agency for Marine-Earth Science and Technology,
Kanagawa, 236-0001, Japan

²Institute of Tibetan Plateau Research, Chinese Academy of Sciences, 100085 Beijing, China

³Meteorological Research Institute, Tsukuba, 305-0052, Japan

⁴National Institute for Agro-Environmental Sciences, Tsukuba, 305-8604, Japan

⁵Hydrospheric Atmospheric Research Center, Nagoya University, Nagoya, 464-8601, Japan

Abstract:

The numerous lakes found throughout the Tibetan Plateau have a large effect on evaporation from the plateau. We analyzed variation in the water cycle in Yamdrok Yumtso Lake basin under the temperature increase of 1.13°C during the 45 years from 1961–2005. Both vapor pressure and relative humidity increased by approximately 17%, resulting in a 13.7% increase in longwave radiation flux and a smaller daily range of surface air temperature. A 5.7% decrease in sunshine duration caused solar radiation flux to decrease by 3%. Heat and water balances were simulated over land and the lake. The lake covers 10% of the total basin area. Evaporation from the lake was larger than that from land, with lake evaporation making up 26% of the basin total. Evaporation from the lake decreased 7% (May–September) over the study period, and observed small pan evaporation also decreased. This trend was not found in the evaporation from land and from precipitation. With water vapor in the air increasing and evaporation from the ground surface (lake and land) decreasing, the water vapor may have come from areas outside the basin and possibly even beyond the plateau.

KEYWORDS Climate change; lake evaporation; Tibetan Plateau; water vapor increase.

INTRODUCTION

Lakes play a key role in continental hydrological cycles. The Tibetan Plateau contains numerous lakes covering a total area of 44,993.3 km², including more than 1091 with individual areas greater than 1.0 km². Most of these lakes are located in sparsely populated areas at elevations over 4000 m. However, the plateau is extremely sensitive to global warming. Satellite images have revealed that the areas of lakes across the plateau have changed in recent years (Lu *et al.*, 2006). The mechanism of the change is still unknown, due to the lack of observational data in this high-altitude region.

Many weather observatories were established on the Tibetan Plateau in the 1950s, and intensive meteorological observations have been conducted in the area since the 1970s. The First Global Atmospheric Research Program (GARP) Global Experiment (FGGE) II-b began upper-air observations in summer 1979. Yanai *et al.* (1992) analyzed FGGE upper-air data and found that

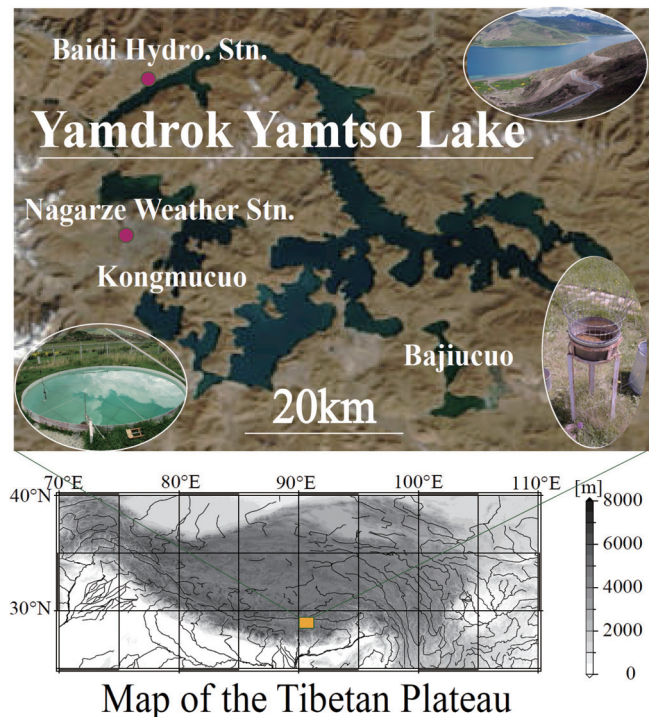


Figure 1. Map of the Yamdrok Yumtso Lake basin (top), Tibetan Plateau (bottom). The photograph in the upper right shows the lake. The large and small pans are shown on the left and right sides, respectively.

sensible heating dominated in early summer, but latent heating dominated during the mid-summer monsoon. The Global Energy and Water Cycle Experiment (GEWEX) Asian Monsoon Experiment (GAME-Tibet) conducted an intensive observation period over Tibet in 1998. Using GAME data, Xu and Haginoya (2001) and Xu *et al.* (2005a) estimated the heat and water balances of daily and seasonal variations over the Tibetan Plateau.

Yamdrok Yumtso Lake (90°41'E, 28°56'N, Figure 1) is one of the three largest lakes of the Tibetan Plateau. Situated 120 km south of Lhasa at 4441 m above sea level, the lake has a catchment area of approximately 6110 km² and surface area of 638 km². Its depth is

Correspondence to: Jianqing Xu, Frontier Research Center for Global Change, Japan Agency for Marine-Earth Science and Technology, Kanagawa, 236-0001, Japan. E-mail: jxu@jamstec.go.jp ©2008, Japan Society of Hydrology and Water Resources.

Received 1 September 2008
Accepted 21 December 2008

unknown. Many snowcapped mountains surround the lake, and numerous small streams feed it. It is almost a closed system; only a small amount of natural runoff flows through a small tributary of the Yarlung-Tsangpo River, with the inflow balanced mainly by evaporation. Kongmucuo Lake and Bajiucuo Lake are independent of Yamdrok Yumtso Lake.

Baidi hydrological station (Figure 1) is located on the lake shore at 90°26′20″E, 29°07′25″N. Evaporation was observed at this station using a large pan. The lake temperature was observed during 1977–1995. Nagarze weather station (ID 55681, 90°24′E, 28°58′N, 4432.4 m) is located 18 km south of Baidi. The air temperature, humidity, and wind speed observed in Nagarze were very similar to those observed at Baidi, and the observation period was longer there.

To reveal the long-term change over the plateau, we used the meteorological data from Nagarze weather station to simulate the evaporation and water temperature of the lake and land. We then compared these estimates with the lake temperature and large pan evaporation that were observed at Baidi station.

DATA SETS AND CALCULATION METHODS

Data sets

Routine meteorological data including daily temperature, humidity, sunshine duration, and wind speed covered 45 years (1961–2005) at the Nagarze Meteorological Station (Table I).

The monthly water temperature and large pan data were acquired from Baidi hydrological station. A large pan (lower left of the upper image in Figure 1) was set up at Baidi. This type of pan is known as a “20 m² basin”; it has a surface area of 20 m², with a diameter of 5 m and depth of 2 m. The evaporation from this type of large pan is nearly the same as the real evaporation of a lake (Brutsaert, 1982), but these pans are costly to install. The large pan was observed from 1984 to 1995 in the warm season (May–September), when 95% of precipitation occurred because of the monsoon climate. Water temperature was measured on one side of the lake from 1977 to 1995.

Calculation methods

The evaporation from three kinds of surfaces was calculated using the same routine meteorological data as input. The surface types were water (lake), soil (land, including snow and frozen processes in winter), and imaginary humid surfaces. Evaporation from land surfaces (represented by E_s in this paper) has been described in detail by Kondo and Xu (1997) and applied to the Tibetan Plateau by Xu and Haginoya (2001) and Xu *et al.* (2005a). Xu *et al.* (2005b) described potential evaporation E_p from an imaginary humid surface. The ratio $WI = Pr/E_p$ was defined as a wetness index (WI) to highlight climatic wetness or dryness, where Pr represents the precipitation.

Estimation of evaporation from a shallow lake

We assumed that the lake was shallow (less than 10 m). A one-layer water model has been produced to

Table I. Statistical amounts during 1961–2005. Observations and calculations are included (column “O/C”). The values in the “Annual” column are the annual amounts, while those in “May–September” are the warm season amounts. The significance level of every trend was tested at $\alpha = 5\%$, with “T” indicating True and “F” indicating False. Changes during the 45 years are also shown. T_{AM} , T_{AMAX} , and T_{AMIN} represent the surface air mean, maximum, and minimum temperature, respectively. N is the sunshine duration, RH is the relative humidity, and V_{pr} is the vapor pressure. Other notations are given in the text. Here, “water” means from the lake, and “soil” means from the land surface.

Item	Unit	O/C	Annual				May–Sept.			
			Mean	Trend yr ⁻¹	Change 45yr	α 5%	Mean	Trend yr ⁻¹	Change 45yr	α 5%
T_{AM}	°C	Obs.	2.8	0.025	1.13	T	8.4	0.013	0.59	T
T_{AMAX}	°C	Obs.	9.7	0.009	0.41	T	14.7	0.002	0.09	F
T_{AMIN}	°C	Obs.	-3.7	0.050	2.25	T	2.8	0.034	1.53	T
U	m s ⁻¹	Obs.	2.6	-0.015	-0.68	T	2.0	-0.010	-0.45	T
N	hour	Obs.	2891.7	-3.659	-164.66	T	1071.3	-1.992	-89.64	T
RH	%	Obs.	42.7	0.159	7.16	T	61.5	0.072	3.24	T
V_{pr}	hPa	Obs.	3.8	0.015	0.68	T	6.8	0.015	0.68	T
S^\downarrow	W m ⁻²	Cal.	246.0	-0.172	-7.74	T	268.7	-0.243	-10.94	T
L^\downarrow	W m ⁻²	Cal.	241.9	0.738	33.21	T	280.0	0.157	7.07	T
Pr	mm	Obs.	358.8	0.548	24.66	F	340.7	0.302	13.59	F
Lpan	mm	Obs.	-	-	-	-	604.2*	-	-	-
SPan	mm	Obs.	-	-	-	-	902.9	-1.446	-65.07	F
E_p	mm	Cal.	1392.5	-2.749	-123.71	T	671.1	-1.064	-47.88	T
WI		Cal.	0.26	0.001	0.05	F	0.51	0.001	0.05	F
Rn (water)	W m ⁻²	Cal.	-	-	-	-	148.6	-0.198	-8.91	T
H (water)	W m ⁻²	Cal.	-	-	-	-	26.0	-0.017	-0.77	F
iE (water)	W m ⁻²	Cal.	-	-	-	-	116.5	-0.184	-8.28	T
Ew (water)	mm	Cal.	-	-	-	-	621.0	-0.975	-43.88	T
Tw (water)	°C	Cal.	7.2	0.0395	1.78	T	14.1	0.023	1.04	T
Tw (obs.)	°C	Obs.	-	-	-	-	14.2**	-	-	-
Rn (soil)	W m ⁻²	Cal.	62.8	-0.068	-3.06	T	91.3	-0.083	-3.74	T
H (soil)	W m ⁻²	Cal.	41.2	-0.079	-3.56	T	48.9	-0.092	-4.14	T
iE (soil)	W m ⁻²	Cal.	20.8	0.004	0.18	F	39.4	-0.004	-0.18	F
E_s (soil)	mm	Cal.	263.2	0.055	2.48	F	208.3	-0.014	-0.63	F
T_s (soil)	°C	Cal.	9.1	0.026	1.16	T	16.4	0.008	0.36	F

*: Averaged from the May–September total amount during 1984–1995.

** : Averaged from the May–September mean amount during 1977–1995.

estimate the evaporation from lakes (Kondo and Kuwagata, 1992).

The downward radiation flux input to the lake can be written as

$$R^\downarrow = (1 - ref)S^\downarrow + \varepsilon L^\downarrow, \quad (1)$$

where R^\downarrow is the input radiation flux, $ref = 0.06$ is the albedo of the water surface, $\varepsilon = 0.98$ is the surface emissivity, S^\downarrow is the solar radiation, and L^\downarrow is the long-wave radiation flux from the atmosphere.

The heat balance equation is written as

$$R^\downarrow - G = \varepsilon\sigma Tw^4 + H + iE, \quad (2)$$

Where

$$G = c_w \rho_w Z \frac{\partial Tw}{\partial t}, \quad (3)$$

$$H = c_p \rho C_H U (Tw - T_{AM}), \quad (4)$$

$$iE = i\rho\beta^* C_H U (hq_{SAT}(Tw) - q_{AM}). \quad (5)$$

Here, G is the heat flux of conduction to the water, σ is the Stefan-Boltzmann constant, and Tw is the calculated water temperature, which satisfies the heat balance equations (Equations (2)–(5)). Sensible and latent heat fluxes H and iE were computed simultaneously. In addition, c_w is the specific heat of water, ρ_w is the density of the water, Z is the depth of the lake, $\partial Tw/\partial t$ is the variation rate of water temperature with time, and c_p and ρ are the specific heat and density of air, respectively. The air temperature is given by T_{AM} , and i is the latent heat of vaporization, with evaporation efficiency $\beta^* = 1$. Finally, $q_{SAT}(Tw)$ is the specific humidity at saturation, q_{AM} is the specific humidity of air, and U is the wind speed. The evaporation rate E under these conditions only takes into account evaporation from the lake.

We used a simple one-layer water model in the present study for several reasons. First, the heat flux conducting into the lake G depended on the temperature change of the lake. The daily range of water temperature was less than the monthly range because of the large thermal physical coefficient of water. Second, the temperature changed at various water depths in different seasons. We assumed depths of 2, 4, 6, 8, and 10 m and performed calculations using these values. Among these five cases, the largest difference in the total evaporation during the warm season (May–September) was 10%, and the largest difference between months was 17%.

The air temperature was lower than 0°C from November to March, and the lake surface froze in winter. However, no observational data were available for winter from the Baidi hydrological station. Therefore, changes in the thermal physical coefficients with freezing and melting processes could not be tested for the freezing season. Hence, we did not consider freezing effects in our model. This omission will not affect the results, because we did not consider evaporation during the cold season in this study.

In Equations (4) and (5), $C_H U$ is the exchange speed. The exchange speed in the bulk formula depends on the evaporation area of a surface. The lake can be treated as a finite water surface area, with averaged width of approximately 3 km (Figure 1). According to Kondo (1994, p. 172), when the wind speed is constant in height over a finite surface, the bulk transfer coefficient for latent heat flux C_E is

$$C_E = 0.2275(\nu/D)^{-2/3}(\log_{10} Re)^{-2.58}, \quad Re : 6.5 \times 10^6 \sim 10^9, \quad (6)$$

$$Re = \frac{XU}{\nu}. \quad (7)$$

where Re is the Reynolds number, ν is the kinematic viscosity coefficient of air, and D is the molecular diffusion coefficient of vapor. We assumed $C_E U \cong C_H U$ and considered the case of natural convection, where $C_H U$ is expressed as

$$C_H U = \max(a + b \times 0.7U, c \times (Tw - T_{AM})^{1/3}), \quad (8)$$

$$a = 0.0023 \text{ ms}^{-1}, \quad b = 0.0025, \quad c = 0.003 \text{ ms}^{-1} \text{ K}^{-3}. \quad (9)$$

Here, a , b , and c were derived from Equations (6) and (7).

Determining the depth of the lake

The depth of the lake was unknown. We assumed depths of 2, 4, 6, 8, and 10 m and calculated heat and water balances with those depths. The minimum $\Sigma[Tw(obs.) - Tw(cal.)^2]$ was found for a depth of 4 m. Therefore, we assumed a lake depth of 4 m.

Figure 2 shows the calculated results (solid lines). The circles are the observed water temperature (upper panel) and large pan evaporation from 1984–1995. The dotted line is the observed small pan evaporation at Nagarze weather station. The simulated values agreed closely with the monthly mean temperature and total evaporation observations in the warm season. The change pattern of the small pan evaporation was similar to that of the large pan and the lake evaporation, but the annual amplitude of the small pan evaporation was the largest.

Figure 2 verifies our one-layer water model of evaporation on the Tibetan Plateau. Evaporation, sensible heat flux, and other quantities relevant to heat and water balances over the lake surface were calculated for 45 years.

RESULTS

Seasonal changes

Figure 3 shows the seasonal variations of the heat and water balances over the lake and land surfaces in the basin. The net radiation R_n into the lake (149 Wm^{-2} , Table I) was much larger than that into the land (91 Wm^{-2}) in the warm season (May–September). This can be explained by the differences in albedo and surface temperature for these two types of surfaces. The

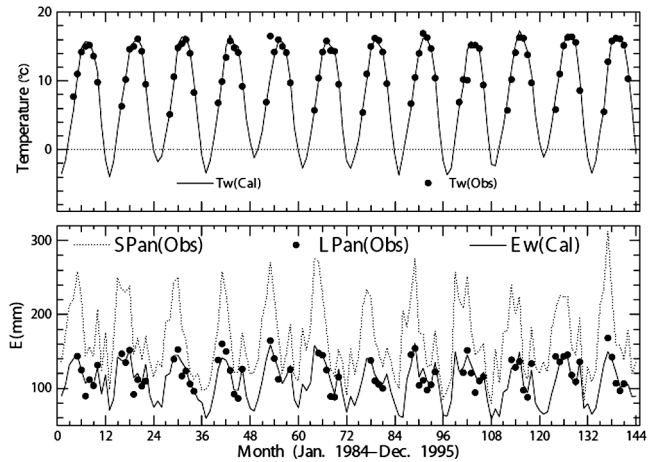


Figure 2. Seasonal changes of the observed water temperature (top) and pan evaporation (bottom). The solid lines and black circles show the calculated results and the observations, respectively. The dotted line shows the observed small pan data.

annual mean surface temperatures of the land and lake were 9.1°C and 7.2°C, respectively, meaning that the upward longwave radiation of the land surface was larger than that of the lake surface. The peak of Rn occurred in May for the lake (Figure 3a) and in August for the land (Figure 3b).

The latent heat flux iE (warm season mean 116 Wm^{-2}) dominated the heat balance over the year on the lake surface. On land, however, sensible heat flux dominated the heat budget in early summer, with iE dominating during the mid-summer monsoon, as in other southeastern parts of the plateau (see Figure 7 of Xu *et al.* 2005a). The land surface temperature Ts (Figure 3c) was highest in early summer, becoming similar to

the lake temperature Tw in the monsoon season due to rainfall Pr (Figure 3e). As noted above, lake area accounts for 10% of the whole basin, and the evaporation from the lake makes up 26% of the basin total; evaporation from the lake (Ew) was 621 mm (Table I) during the warm season, which far exceeded the precipitation of 341 mm, while evaporation from the land surface was 208 mm (Figure 3d). The seasonal change of small pan evaporation (SPan) was similar to that of the lake and to large pan (LPan) evaporation. However, the difference between SPan and LPan was larger in early summer. August was the most humid month, with WI over 1.0 (Figure 3e). The soil water content generally followed the precipitation changes (Figure 3f), in agreement with previous findings for the southeastern area (see Figure 7f of Xu *et al.*, 2005a)

Long-term variation

Over the study period, the basin had an average pressure of 591 hPa and vapor pressure of 3.85 hPa, just one third that of Tokyo. Figure 4 shows long-term changes in heat and water balances from 1961 to 2005. The increase in temperature of 1.13°C (Figure 4a, Table I), combined with the vapor pressure Vpr (Figure 4c) increase of 0.68 hPa (17.5%) and the 7.16% (16.8% in 45 years) increase in relative humidity RH (Table I), resulted in downward longwave radiation flux L^{\downarrow} increasing by 33.21 Wm^{-2} (13.7%, Figure 4f) during the 45-year period. The decreased sunshine duration (Figure 4b) reduced the downward solar radiation flux S^{\downarrow} (Figure 4e).

The same trends were found on an annual basis and for the warm period (May–September). In the warm season (May–September), evaporation from the lake E_w (Figure 4h) decreased 43.88 mm (7%), a result that corresponded to the decrease in SPan (Figure 4g). This decrease can be explained by the increase of q_{AM} (Equation (5)), which is directly proportional to Vpr . The decrease in the daily air temperature range ($\Delta T_{AMIN} \gg \Delta T_{AMAX}$, Table 1) would have resulted from the decrease in radiative cooling (L^{\downarrow}). Precipitation Pr (Figure 4j) increased slightly, and evaporation from the land surface Es (Figure 4i) barely changed; however, the reliabilities of these trends were not significant (Table I). The basin is located in a semi-arid climate region with $WI = 0.26$; the land surface is not always sufficiently wet, therefore, Es mainly depended on Pr , and most of the precipitation (approximately 60%) evaporated annually. Although WI (Figure 4k) increased, the increase was not significant.

SUMMARY AND CONCLUDING REMARKS

We successfully used a one-layer water model, multi-layer soil model, and potential evaporation method to simulate long-term changes in heat and water balances for the land and lake areas of the Yamdrok Yumtso Lake basin. Warming has been confirmed in this region. For the water cycle under this warming condition, we found that both vapor pressure and relative humidity increased in the basin. These increases resulted in an increase in the longwave radiation flux and reduction in the daily temperature range. Evaporation from the lake made up approximately 26% of the total amount of evaporation in the basin; over the study period, lake evaporation decreased 7% (May–September), a trend that was not found in evaporation from land and from precipitation, which showed no significant change. Given the increase in water vapor in the air (Vpr and RH) and the decrease of evaporation from the ground

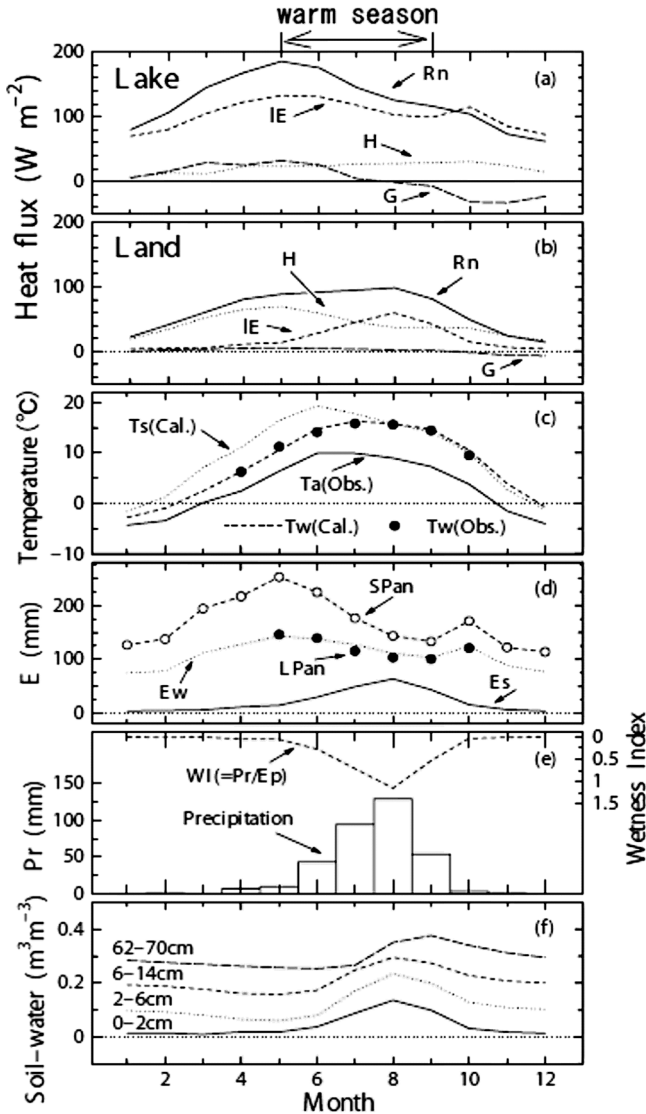


Figure 3. Monthly variations of the heat balance and water balance of the basin. Heat fluxes over (a) the lake's surface and (b) land surface. (c) Land surface temperature Ts (dotted line), water temperature Tw (the dashed line and black circles show the calculated values and the observations, respectively), and observed air temperature (solid line). (d) Observed SPan evaporation (dashed line with open circles), LPan evaporation (black circles), and calculated evaporation from the lake Ew and land surface Es . (e) Precipitation Pr and wetness index WI . (f) Volumetric soil water content for four layers.

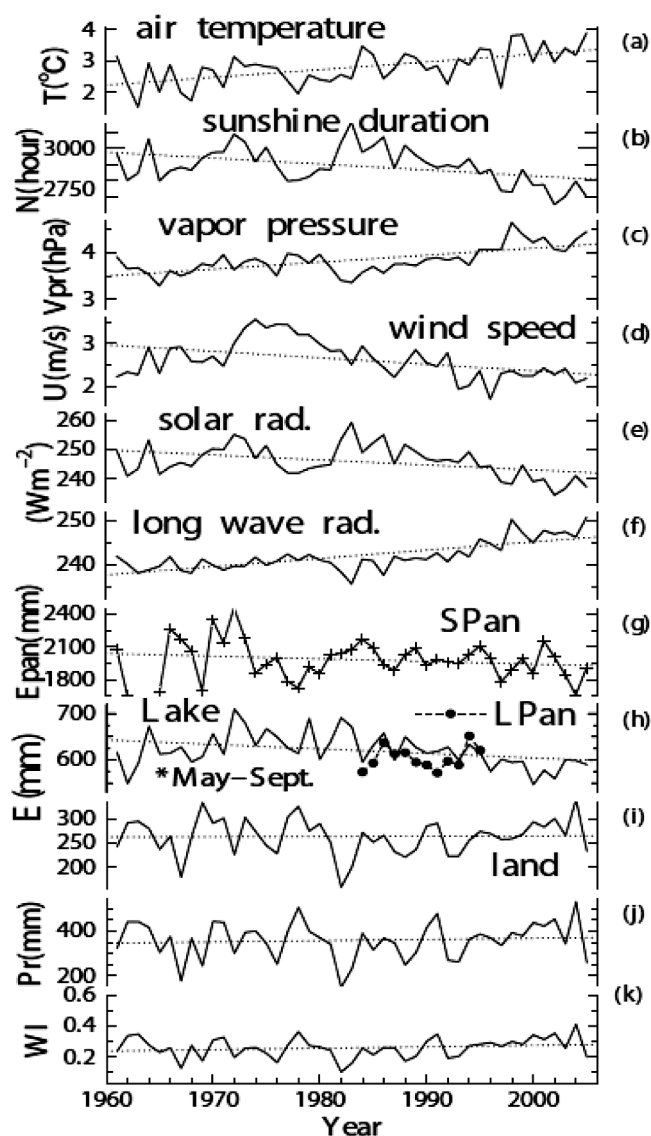


Figure 4. Interannual variations (solid lines) for the basin from 1961 to 2005. Dotted lines represent the trends obtained by linear regression. (a) Air temperature, (b) sunshine duration, (c) vapor pressure, (d) wind speed, (e) solar radiation flux, (f) longwave radiation flux, (g) small pan evaporation, (h) evaporation from the lake and large pan (black circle with dashed line), (i) evaporation from the land surface, (j) precipitation, (k) WI.

surface (sum of lake E_w and land E_s), it is possible that the water vapor originated outside the basin and maybe even outside the plateau. Future research will analyze long-term change in large-scale weather conditions around the plateau.

ACKNOWLEDGEMENTS

We thank Dr. Yuping Yan of the China Meteorological Administration. We also thank the Climate Center of the China Meteorological Administration and the Hydrological Bureau of Tibet for providing the data. Thanks are also extended to Prof. Fujio Kimura and Dr. Rikie Suzuki of FRCGC, JAMSTEC. This project was supported by JSPS and China NSFC (No. 40571037 and No. 40711140130) under the Japan-China Scientific Cooperation Program. DIAS was used to prepare the data.

SUPPLEMENTS

Supplement 1 Enlarged figure of Figure 1 is included.
 Supplement 2 Enlarged figure of Figure 2 is included.
 Supplement 3 Enlarged figure of Figure 3 is included.
 Supplement 4 Enlarged figure of Figure 4 is included.

REFERENCES

- Brutsaert W. 1982. *Evaporation into the Atmosphere*. D. Reidel Publishing Company, Holland; 299 pp.
- Kondo J. 1994. *Meteorology of the Water Environment - Water and Heat Balance of the Earth's Surface*. Asakura Shoten Press, Japan; 348 pp. (in Japanese).
- Kondo J, Kuwagata T. 1992. Hydrological climate in Japan (1): Radiation and evaporation from shallow lakes. *Journal of Japan Society of Hydrology and Water Resources* 5: 13-27 (in Japanese with English summary).
- Kondo J, Xu J. 1997. Seasonal variations in the heat and water balances for nonvegetated surfaces. *Journal of Applied Meteorology and Climatology* 36: 1676-1695.
- Lu A, Wang L, Yao T. 2006. The study of Yamzho Lake and Chencuo Lake variation using remote sensing in Tibet Plateau from 1970 to 2000. *Remote Sensing Technology and Application* 21: 173-177 (in Chinese with English summary).
- Xu J, Haginoya S. 2001. An estimation of heat and water balances in the Tibetan Plateau. *Journal of the Meteorological Society of Japan* 79(1B): 485-504.
- Xu J, Haginoya S, Masuda K, Suzuki R. 2005a. Heat and water balance estimates over the Tibetan Plateau in 1997-1998. *Journal of the Meteorological Society of Japan* 83: 577-593.
- Xu J, Haginoya S, Saito K, Motoya K. 2005b. Surface heat balance and pan evaporation trends in eastern Asia in the period 1971-2000. *Hydrological Processes* 19: 2161-2186, DOI: 10.1002/hyp.5668.
- Yanai M, Li C, Song Z. 1992. Seasonal heating of the Tibetan Plateau and its effects on the evolution of the Asian summer monsoon. *Journal of the Meteorological Society of Japan* 70: 319-351.